One-step deposition of Au nanoparticles onto chemically modified ceramic hollow spheres via self-assembly

Begum, S, Jones, IP, Lynch, DE & Preece, JA

Original citation & hyperlink:
Begum, S, Jones, IP, Lynch, DE & Preece, JA 2012, 'One-step deposition of Au nanoparticles onto chemically modified ceramic hollow spheres via self-assembly' *Journal of Experimental Nanoscience*, vol 7, no. 1, pp. 1-16
https://dx.doi.org/10.1080/17458081003752962

DOI 10.1080/17458081003752962
ISSN 1745-8080
ESSN 1745-8099

Publisher: Taylor and Francis

This is an Accepted Manuscript of an article published by Taylor & Francis in Journal of Experimental Nanoscience on 17th October 2011, available online: http://www.tandfonline.com/10.1080/17458081003752962

One step deposition of Au nanoparticles onto chemically modified ceramic hollow spheres *via* self-assembly

Shakiela Begum,[a] Ian P. Jones,[b] Daniel E. Lynch*[c] and Jon A. Preece*[a]

[a] *School of Chemistry, University of Birmingham, Edgbaston, Birmingham, B15 2TT, UK. Fax: +44(0)121 414 4403; Tel: +44(0)121 414 3528; E-mail: sxb398@bham.ac.uk and j.a.preece@bham.ac.uk*
[b] *Department of Metallurgy and Materials, University of Birmingham, Edgbaston, Birmingham, B15 2TT, UK. FAX: +44(0)121 414 5232; Tel: +44(0)121 414 5184; E-mail: i.p.jones@bham.ac.uk*
[c] *Exilica Limited, The Technocentre, Puma Way, Coventry, CV1 2TT, UK.; Tel: +44 (0)24 7688 8505; E-mail: d.lynch@exilica.co.uk*

* Corresponding authors

(Received 20 July 2005; final version received 17 August 2006)

A concentrated citrate stabilised Au nanoparticle (NP) colloid has been prepared using a modified Frens procedure, and characterised using TEM and UV-vis absorption spectroscopy. The average diameter determined from TEM images of concentrated Au NPs (16.57 ± 0.65 nm) is similar to the diameter reported by Frens (16 nm). The surface plasmon band of the concentrated Au NPs UV-vis spectrum has a λ_{max} at 522 nm. Bare silica and iron-silica hollow microsphere surfaces have been functionalised with amino groups using the surfactant 3-aminopropyltrimethoxysilane (APTMS). The Au NPs have been assembled onto the APTMS treated hollow spheres by dispersing a colloid of Au NPs into a suspension of hollow spheres at pH 4.5 (2 hrs). The volume ratio of Au NPs:hollow spheres was adjusted until maximum deposition could be achieved in a single step. TEM micrographs of ultrathin (80-100 nm) ultramicrotome sections through the Au NP coated hollow spheres reveal that a single layer of Au NPs is mainly distributed on (i) the external side of the shell wall for silica, and (ii) both sides of the shell wall for iron-silica. UV-vis absorption spectra of the Au NP coated hollow spheres show that the surface plasmon band shifts (524-613 nm) and broadens as the density of Au NPs is increased on the shell surface.

Keywords: concentrated gold nanoparticles; 3-aminopropyltriethoxysilane (APTMS); silica and iron; hollow spheres; TEM of ultramicrotome sections

1. Introduction

The design of gold nanoparticle (Au NP) and silica sphere composites is application driven. Examples of application areas include biomedical (*i.e.* drug delivery, cell labelling, and cell destruction) [1], catalysis [2], and sensors (*i.e.* opal structures) [3]. As seen from the publications in this area a variety of approaches have been used to prepare Au-silica composites [1-29]. There are papers dedicated to adsorbing Au NPs inside [2-11], outside [12-25], or both sides [25-27] of silica spheres. The surface of

the silica or template would usually be chemically modified to allow the assembly the Au NPs or $AuCl_4^-$ precursors onto the surfaces of the spheres [29]. The advantage of using hollow spheres instead of dense beads is that the hollow spheres have a higher surface area, and a greater capacity to adsorb higher amounts of Au NPs.

The advantage of having Au NPs or a Au phase on the internal side of the silica hollow sphere is that the silica will serve as a protective coating over the Au, while the porosity of the silica will allow chemicals to diffuse inside. Au NPs can be distributed on the internal surface of a hollow sphere using different methods, *i.e.* reduction of $HAuCl_{4\ (aq)}$ on the inside silica hollow spheres [4], preparation of sacrificial core-Au NP-silica or silica core-Au NP-silica composite [2, 5, 6], Au NPs interdispersed inside the silica shell [9], or Au-silica core-shell NPs have been assembled on polystyrene spheres [10]. However, the extent of Au NP coverage achieved by these methods is not high.

There are three main routes for preparing Au coated silica hollow spheres, (i) direct deposition of Au NPs by mixing two colloids [12-18], (ii) *in situ* reduction of $HAuCl_4$ [21], or (iii) deposition of Au NPs that act as "seeds" for the further growth of the Au shell from exposure to $HAuCl_{4\ (aq)}$ [19, 22, 24]. The disadvantage of some of the current methods using route (i) is that the silica sphere is repeatedly exposed to colloidal Au and the unreacted Au NPs are washed out in order to gain dense coverage. This process can be time consuming and expensive. Some studies have shown that Au NP coverage on the outer surface of silica can be improved when the pH of the reaction is adjusted [13-15, 19, 24]. Furthermore, Osterloh *et al.* showed that citrate stabilised Au NPs desorb from amine functionalised silica spheres when the Au-silica composite is exposed to dilute HCl or KBr (0.1M) [15].

Aside from Au-silica composites there is also interest in preparing multifunctional Au-silica-Fe composite spheres [30-37]. Au-silica-Fe composite spheres are useful as magnetic drug delivery vectors or catalyst supports [32]. These type of structures can be built layer-by-layer (LBL) [33-36], or by covering the silica surface with a single layer made up of Au and iron oxide [30, 31]. The LBL approach involves coating the iron oxide based magnetic NPs with a layer of either silica, followed by an over coat of Au NPs [34-36], or Au-silica core-shell NPs [33]. The Au layer may adsorb by seeded growth [31, 34, 35], or direct deposition of Au NPs [30].

Papers demonstrating high single Au NP coverage concern silica particle sizes in the range 100-500 nm [13-15, 19]. For large particles (> 1 μm) the coverage of the silica surface is incomplete, unless the Au nanoshell is formed *via* seeded growth [19, 22, 24]. Dense Au NP coverage of the silica surface is beneficial, as a maximum number of Au NP sites will be available and the Au-silica composite would become more effective in its application.

Here we aim to demonstrate a procedure to coat amine functionalised silica and Fe-silica hollow spheres with a single uniform sub-monolayer of Au NPs (at pH 4.5). Maximum deposition of Au NPs was achieved in a single step by virtue of using a concentrated citrate stabilised Au sol. Au NPs were loaded onto the internal and external surfaces of the Fe-silica, and only the external surface for the majority of the silica hollow spheres. The Au NP decorated hollow spheres have been characterised by TEM and UV-vis to show the morphology and surface plasmon response. The work presented here describes a novel one-pot methodology for achieving the highest loading of Au NPs on hollow spheres, allowing access to various potential applications [1-3]. Also, there are no reports to our knowledge demonstrating the

adsorption of Au NPs onto Fe-silica hollow spheres, with potential application in magnetic drug delivery [32].

2. Experimental

2.1 Materials

The following chemicals were supplied by Sigma-Aldrich, 3-aminopropyltriethoxysilane (APTMS), trisodium citrate, chloroform, and gold (III) chloride trihydrate. The following chemicals and materials were supplied by Fisher, ethanol, hydrochloric acid, sodium hydroxide, and sodium chloride, and disposable UV-vis cuvettes with four clear sides. The silica ('Si') and iron oxide-silica ('FeSi') hollow spheres were supplied by Exilica [38]. Ultra pure water (UPW) had a resistivity of 18 MΩcm. The chemicals and materials used for SEM and TEM experiments were purchased from Agar Scientific. All the chemicals and materials were used as received.

2.2 Immobilisation of Au NPs onto APTMS treated hollow spheres

2.2.1 Preparation of APTMS coated 'Si' hollow spheres

Dry hollow 'Si' spheres (100 mg) suspended in anhydrous ethanol (10 ml) were stirred under a $N_{2\,(g)}$ atmosphere for 20 minutes. Liquid APTMS (0.487 mmol, 85 µL) was added to the suspension (using a micropipette) and heated under reflux for 24 hrs. The suspension was cooled and left to stir (1 hr). The suspension was transferred to a centrifuge tube (50 ml), and was centrifuged at 3500 rpm (10-15 minutes), and the supernatant syringed off. The APTMS coated 'Si' particles were resuspended, sequentially in ethanol (40 ml (x1)), chloroform (40 ml (x1)), ethanol (40 ml (x2)), and UPW (40 ml (x1)) and centrifuged, syringing off the solution each time. Finally the 'Si' particles were resuspended in UPW (5 ml) and stored until further use.

2.2.2 Preparation of APTMS coated 'FeSi' hollow spheres

The 'FeSi' hollow spheres were coated with APTMS using exactly the same procedure used for the 'Si' spheres.

2.2.3 Preparation of concentrated Au NPs

A $HAuCl_{4\,(aq)}$ solution (50 ml, 0.08 wt%) was heated to reflux and Na_3-citrate $_{(aq)}$ solution (1 ml; 0.8 wt%) was added. The colour of the clear reaction mixture changed from yellow to grey to a deep maroon colour in a matter of seconds. The reaction mixture was heated under reflux (6 minutes). The colloidal suspension was cooled, and centrifuged at 3500 rpm (5 minutes). The supernatant was syringed off. The Au colloid was centrifuged once more, and the supernatant syringed off. This process was repeated once more. The supernatant containing the particles was kept.

2.2.4 Attachment of Au NPs onto APTMS-'Si' hollow spheres

The Au sol (0.66 ml,

Table 1) was added to the APTMS-'Si' suspension (0.5 ml) with stirring. The pH of the reaction mixture was reduced to 4.5 using HCl (100 mM, 10-100 μL portions). The reaction mixture was left to stir (2 hrs). The Au-APTMS-'Si' particles were centrifuged (3500 rpm, 15 minutes) suspended in UPW (45 ml, (x3)). The centrifuge washings were tested (surface plasmon band) for Au NPs by UV-vis. The washed Au- APTMS-'Si' particles were resuspended in UPW (30 ml) and tested by UV-vis. The Au- APTMS-'Si' particles were isolated by centrifuge and dried by vacuum overnight.

2.2.5 Attachment of Au NPs onto APTMS-'FeSi' hollow spheres

Au NPs were attached to the APTMS-'FeSi' hollow spheres using the same procedure used for the APTMS-'Si' hollow spheres. Table 2 summarises the amounts of colloidal Au reacted with colloidal APTMS-'FeSi' hollow spheres (0.5 ml).

2.3 Zeta-potential of the APTMS treated hollow spheres

2.3.1 Sample preparation

The APTMS treated hollow sphere aqueous suspension (1 ml) was diluted with UPW (30 ml). An aliquot (1 ml) of the suspension was dispersed in aqueous NaCl (100 mM, 10 ml). The pH of the dispersion was modulated by addition of aliquots of aqueous HCl (10-100 μL, 10 mM) or NaOH (10-100 μL, 10 mM), to yield suspensions with pHs between 3.5-9.0 in increments of 0.5. Bare hollow spheres (~ 10-20 mg) dispersed in UPW (20 ml) at pH 6 were also characterised.

2.3.2 Zeta-potential

Zeta potential measurements were recorded using a Malvern Instruments Zetasizer 1000Hs, operating with a variable power (5-50 mW) He-Ne laser at 633 nm.

2.4 SEM characterisation of 'Si' hollow spheres

2.4.1 Sample preparation

Bare 'Si' (10 μL from a suspension of ~ 10 mg 'Si':1 ml UPW) or APTMS-'Si' hollow spheres suspended in UPW (10 μL) were placed on a glass cover slip mounted on an SEM stub using double sided carbon tape. The SEM stub was left to stand in air to allow the water to evaporate. The edges of the cover slip were painted with silver paint and the stub was coated with carbon by thermal evaporation using an Edwards 306 coating unit.

2.4.2 Scanning Electron Microscope

Secondary images of the bare 'Si' and APTMS-'Si' hollow spheres were acquired using a JEOL 7000 FEG SEM set at an acceleration voltage of 4 kV.

2.5 TEM characterisation of the Au NPs and hollow spheres

2.5.1 Preparation of the Au NP TEM grid

The concentrated Au sol was diluted by a factor of eight. The dilute Au colloid (5 μL) was placed on a formvar coated copper grid for one minute. The excess Au colloid dispersion was removed by adsorbing onto a filter paper.

2.5.2 Preparation of the specimen block: addition of specimen to resin

The araldite resin was formulated from Araldite CY212 (3 ml), EPON substitute Agar 100 RESIN (5 ml), DDSA (hardner, 13 ml) and DBP (plasticiser, 0.6 ml) via stirring for 5 minutes. The liquid accelerator (DMP 30, 0.5 ml) was added to the mixture while stirring resulting in a colour change from yellow to orange. The mixture was placed under vacuum (20 minutes, 23 °C). Two beam capsules (20 mm x 9 mm) were completely filled using a syringe (5 ml) containing the air free resin. The powdered specimen (~0.5-1 mg) was added to each resin filled beam capsule, and the mixture inside the capsule was gently agitated to help the shells sink into the resin. The beam

capsules were heated (60 °C) under vacuum (30 minutes). The resin was left to cure (60 °C) at ambient pressure overnight to yield a polymerised resin-specimen block.

2.5.3 Preparation of ultramicrotome sections of Au NP coated hollow spheres

The Araldite specimen blocks were trimmed by hand using a double-sided razor blade until the cutting face was pyramidal shaped and the hollow spheres were exposed and within the trapezoid-shaped pyramid top. The block was secured into a REICHERT-JUNG ultramicrotome, and was fine trimmed using a glass knife set at a clearance angle of 4°. The glass ultramicrotome knife was prepared by breaking a glass strip (1 cm thick) using a knife maker (type 7801A). Ultrathin (80-100 nm) sections of the block were obtained using a diamond knife set at a clearance angle of 6°. The gold coloured sections were captured onto formvar coated grids by sweeping the section out of the water.

2.5.4 Transmission Electron Microscope

TEM bright field micrographs were obtained using the JEOL 1200EX TEM set at an acceleration voltage of 80 kV.

2.6 UV of Au NPs, centrifuge washings and Au NP coated hollow spheres

2.6.1 Sample preparation

The concentrated Au NP colloid was diluted by a factor of two using UPW [39]. The centrifuge washings were tested by UV as prepared. The Au coated hollow spheres in UPW (30 ml) were agitated and immediately transferred to a cuvette and tested without delay because most of the hollow spheres were aggregated and showed a tendency to sediment over time [40].

2.6.2 UV-vis spectrometer

UV-visible absorption spectra of the colloidal Au and the suspensions of Au coated hollow spheres were obtained using a Hewlett Packard 8452A spectrometer (wavelength range= 400-800 nm).

3. Results and Discussion

3.1 Preparation of Au NP coated hollow spheres

The overall process for the assembly of the citrate passivated Au NPs onto the hollow spheres is shown in Scheme 1. The bare hollow spheres were coated with a self-assembled monolayer (SAM) of APTMS from an anhydrous ethanol solution (Figure 1), using a modified procedure by Badley *et al.*[41] The suspension of 'Si' hollow spheres in ethanol was heterogeneous initially, *i.e.* the powder was caked and grains were floating in the dispersant. The 'FeSi' hollow spheres were less heterogeneous before treatment with APTMS. The APTMS hollow sphere dispersions formed by prolonged (24 hours) stirring under reflux produced a more homogenous dispersion than without APTMS. The APTMS coated hollow spheres were also easier to disperse after sedimentation. APTMS treated hollow spheres were washed successively with ethanol, chloroform, and ethanol to remove the excess APTMS and were finally transferred into UPW (5 ml). The hollow spheres are partially ruptured when the organic template is removed by calcination [38, 40], therefore, the inner surface of the spheres should also be coated with an APTMS SAM (see later). The predominant phase of the 'FeSi' hollow spheres is silica [40], therefore, it was possible to assemble an APTMS monolayer onto the 'FeSi' hollow spheres using the same chemistry used for the 'Si' hollow spheres. The first reaction in Scheme 1 is a depiction of the reaction between APTMS and the hollow spheres. The APTMS treated hollow spheres were then suspended in 100 mM $NaCl_{(aq)}$, the pH was modified over a pH range of ~ 3-9, and the zeta-potential was monitored (Figure 2).

Au NPs were prepared by a modified Frens [42] procedure to afford a concentrated [43] colloidal suspension. The colloidal Au NP suspension was then added to the colloidal suspension of APTMS treated hollow spheres (‘Si’ and ‘FeSi’) using several ratios (

Table 1 and Table 2), and the pH was adjusted to pH 4.5. The pH was reduced in order to protonate the APTMS SAM to make it positively charged, and hence promote the electrostatic assembly of negatively charged Au NPs [44]. The ratio of the hollow spheres:Au NPs was adjusted systematically until the Au NPs were in excess as noted by the resulting supernatant having Au NPs present. Thus, we reached a situation in which a maximum surface coverage of the Au NPs on the hollow surface was observed. The excess citrate present in the Au was not removed because other authors [16] have shown that the presence of excess citrate in the Au colloid assists the self assembly process of the Au NPs onto amine functionalised silica beads. Ultramicrotome sections through the Au NP coated hollow spheres (Au-APTMS-'Si' and Au-APTMS-'FeSi') embedded in Araldite resin were prepared and imaged using TEM (Figures 4-6), and UV-vis spectra of suspensions of Au NP coated hollow spheres in UPW were recorded (

Table 1, Table 2 and Figure 7).

3.2 Characterisation of the Au NP coated hollow spheres

3.2.1 SEM characterisation of APTMS coated hollow 'Si' spheres

The APTMS-'Si' hollow spheres were examined using low voltage (4 kV) SEM. JEOL 7000 FEG SEM images of carbon coated (a) bare 'Si' and (b) APTMS-'Si' hollow spheres are shown in Figure 1. From these SEM images we can see that the surface morphology of the 'Si' hollow spheres does not significantly change after treatment with APTMS.

3.2.2 pH dependent zeta potentiometry study of APTMS coated hollow spheres

A plot of zeta potential (mV) vs. pH for dilute suspensions of (a) APTMS-'Si' and (b) APTMS-'FeSi' hollow spheres in UPW (1 ml) dispersed in NaCl solution (100 mM, 10 ml) is shown in Figure 2. The zeta-potential results from this study (Figure 2) show that the APTMS-'Si' and APTMS-'FeSi' coated hollow spheres are positively charged and are electrostatically stable in the pH range of 3.5-6.5 and 3.5-5.5, respectively. Further increase of the pH caused a reduction in the zeta-potential and the conjugate bases are protonated. Interestingly the APTMS-'FeSi' hollow spheres display significantly different behaviour at high pH than the APTMS-'Si' spheres. Presumably the iron phase chemistry is playing some pH dependent role. The bare 'Si' hollow spheres dispersed in UPW have a zeta-potential of -39.4 mV, and the 'FeSi' hollow spheres: -38.2 mV (pH 6).

3.2.3 Determination of the average diameter of concentrated Au NPs by TEM

Frens showed (TEM) that Au NPs prepared using $HAuCl_4$ (0.01 wt%, 50 ml) and trisodium citrate (0.1 wt%, 1 ml) have an average diameter of 16 nm [42]. In this study bright field TEM micrographs have been statistically analysed to determine the average diameter of the Au NPs prepared here using a modified route to produce a

significantly more concentrated dispersion. A bright field TEM micrograph of the concentrated Au NPs is shown in Figure 3a. The TEM image shows that the particles are spherical and relatively monodisperse in size. A histogram of frequency vs. diameter (nm) of the Au NPs is shown in Figure 3b. The average diameter of the colloidal Au NPs is 16.57 ± 0.65 nm (n = 105) [45], which is in good agreement with the diameter reported by Frens (16 nm) [42].

3.2.4 UV-vis of the concentrated Au NP colloid

The λ_{max} of the surface plasmon band of the Au NPs is 522 nm which is within the expected range of 520-525 nm [46, 47] for citrate passivated Au NPs. There was no evidence of the longitudinal band at longer wavelengths, suggesting the NPs were not aggregated [47].

3.2.5 TEM characterisation of Au-'Si' hollow spheres

TEM images of ultramicrotome sections (Figure 4) show: (i) Au NPs adsorb onto APTMS-'Si' hollow spheres at pH 4.5 (Figures 4-5), (ii) the density of the Au NPs on the Au-APTMS-'Si' surface increases with increase in the volume of the Au NP dispersion, and (iii) most of the Au NPs adsorb onto the outer side of the Au-'Si' sphere wall.

A minority of the APTMS-'Si' spheres had Au NPs assembled onto the inner surface (Figure 5), but only at the relatively high Au NP loading (Au-'Si'$_D$,

Table 1). Thus, the APTMS SAM presumably does form on the inner surface of some of the hollow spheres. It is not clear at this point as to whether this low degree of assembly of the Au NPs to the inner surface is due to (i) poor SAM formation on the inner surface, or (ii) the inability of the Au NPs to pass through the rupture in the hollow sphere.

3.2.6 TEM characterisation of Au-APTMS-'FeSi' hollow spheres

Initially the volume ratio of APTMS-'FeSi':Au NPs colloid was the same as the ratio used for specimen Au-'Si'$_D$ (Table 1). Bright field micrographs of specimen Au-'FeSi'$_E$ (Table 2) are shown in Figures 6a and 6b, and show that the majority of the Au NPs attach to the Au-'FeSi' hollow spheres in a similar way to specimen Au-'Si'$_D$ (Figure 4d), *i.e.* to the outer surface only. For both cases (Figure 6a and Figure 4d) we can see the Au NPs are densely packed on the outer surface of the shell, and a few examples were found of hollow spheres where the Au NPs have adsorbed onto the internal surface.

Further increase in the volume of Au NP dispersion (Au-'FeSi'$_F$, Table 2) in the reaction mixture yields hollow spheres coated with the highest density of Au NPs on the outer surface, and increasingly coated internal surfaces (Figures 6c and 6d). Figures 6a-6d suggest that the Au NPs assemble onto the outer surface initially as with the Au-APTMS-'Si' system. Evidence from the Au NPs on APTMS-'Si' experiments showed that when the reaction mixture is saturated with Au NPs it is an indication that the maximum number of Au NPs have attached onto the shell surface. 40 ml of Au NP colloid (Au-'FeSi'$_G$, Table 2) is required to saturate the Au-APTMS-'FeSi' reaction mixture (more than twice the amount required for specimen Au-'Si'$_D$,

Table 1), presumably due to the internal inner structures resulting in a large surface area. TEM images (Figures 6e and 6f) of the specimen Au-'FeSi'$_G$ (Table 2) show that the density of Au NPs immobilised inside the Au-APTMS-'FeSi' hollow spheres is similar to that on the outer shell surface. Figures 6c-6f also suggest that the APTMS monolayer coated the internal surface of the shell as illustrated in Scheme 1.

The TEM images (Figures 4-6) also show that the Au NPs do not coalesce and form a sub-monolayer due to the electrostatic repulsion between charged Au NPs on the hollow sphere surface.

3.2.7 UV-vis spectra of Au coated hollow spheres

The UV-vis spectra of the Au-APTMS-'Si' and Au-APTMS-'FeSi' systems as a function of the volume of the Au NP solution that was added are shown in Figures 7a and 7b. Also plotted is the UV-vis spectrum of the initial colloidal Au dispersion with the λ_{max} of the surface plasmon at 522 nm. Clearly, it can be observed that as the volume of the Au NP colloidal dispersion was increased there is a significant shift and broadening of the Au NP surface plasmon band. The Au-APTMS-'Si' system shifted 48 nm to 570 nm (

Table 1), and the Au-APTMS-'FeSi' system shifted 91 nm to 613 nm (Table 2). These shifts are indicative of dipole-dipole coupling of neighbouring Au NPs, the shift being dependent proportionate to the separation of the Au NPs [2, 10, 16]. These shifts are in good agreement with the TEM analysis where the average Au NP separation decreases as the volume of the Au NP colloidal dispersion increases. In addition no longitudinal band at > 700 nm appeared, supporting the TEM results that the Au NPs were not coalesced. Furthermore, it should be noted that repeated washing of the Au-APTMS-'Si' and Au-APTMS-'FeSi' composite systems with water did not remove any of the assembled Au NPs from the sphere surfaces, as evidenced by no surface plasmon band appearing in the supernatant washings.

4. Conclusion

A concentrated citrate Au NP colloid has been prepared using a modified Frens procedure, and characterised using TEM and UV-vis absorption spectroscopy. The average diameter determined from TEM image analysis of concentrated Au NPs (16.57 ± 0.65 nm) is similar to the average Au NP diameter (16 nm) reported by Frens. The λ_{max} (522 nm) of the concentrated Au NPs falls into the typical range (520-525 nm) usually observed for Au NPs with diameters 16-20 nm. Bare 'Si' and 'FeSi' hollow spheres have been functionalised with an APTMS SAM. Low voltage (4 kV) SEM images of carbon coated bare 'Si' and APTMS-'Si' showed that treatment of the hollow spheres with APTMS does not lead to significant changes in surface morphology. A pH study of the APTMS treated hollow spheres using zeta-potential measurements revealed that the hollow spheres are positively charged in the pH ranges 3-6.5 (APTMS-'Si') and 3.5-5.5 (APTMS-'FeSi') and the surface charge decreases above pH 6.5 (APTMS-'Si') or 5.5 (APTMS-'FeSi'). Au NPs have been assembled onto the hollow spheres by mixing a colloid of Au NPs with a colloid of

APTMS treated hollow spheres at pH 4.5. The assembly appeared to take place in a two stage process whereby the Au NPs assemble onto the outer surface first and then the inner surface. However, the majority of the APTMS-'Si' internal surfaces are not covered by the Au NPs and this raises the question as to whether the APTMS SAM has not formed efficiently on the inner surfaces, or the Au NPs cannot pass through the rupture in the shell surface. Once the particles have been immobilised onto the hollow spheres they do not detach from the shell surface when resuspended in fresh UPW. TEM micrographs of ultrathin (80-100 nm) ultramicrotome sections through the Au NP coated hollow spheres reveal that a single sub-monolayer of Au NPs is mainly distributed on (i) the external side of the shell wall for Au-APTMS-'Si', and (ii) both sides of the shell wall for Au-APTMS-'FeSi'. UV-vis absorption spectra corroborate the increased density of Au NPs on both sets of hollow spheres (TEM), as the surface plasmon band both shifts to higher wavelengths and broadens, showing coupling of the surface plasmons. Such composite materials have a variety of potential applications ranging from catalytic reactors to drug delivery [1, 2, 32].

Acknowledgements

This work was supported by EPSRC and the following Schools at the University of Birmingham: Chemistry, Metallurgy and Materials and Chemical Engineering. The hollow sphere specimens were supplied by Exilica. In addition, the work was carried out under the Science City Project: Innovative uses of materials for a modern world funded by Advantage West Midlands and the ERDF.

References and Notes

[1] L. R. Hirsch, A. M. Gobin, A. R. Lowery, F. Tam, R. A. Drezek, N. J. Halas and J. L. West, *Metal nanoshells*, Ann. Biomed. Eng., 34 (2006), pp. 15-22.

[2] I. Pastoriza-Santos, J. Perez-Juste, S. Carregal-Romero, P. Herves and L. M. Liz-Marzan, *Metallodielectric hollow shells: Optical and catalytic properties*, Chem. Asian J., 1 (2006), pp. 730-736.

[3] T. Nakamura, Y. Yamada and K. Yano, *Direct synthesis of monodispersed thiol-functionalized nanoporous silica spheres and their application to a colloidal crystal embedded with gold nanoparticles*, J. Mater. Chem., 17 (2007), pp. 3726-3732.

[4] W. S. Choi, H. Y. Koo and D. Y. Kim, *Facile fabrication of core-in-shell particles by the slow removal of the core and its use in the encapsulation of metal nanoparticles,* Langmuir, 24 (2008), pp. 4633-4636.

[5] X. W. Lou, C. L. Yuan, E. Rhoades, Q. Zhang and L. A. Archer, *Encapsulation and Ostwald ripening of Au and Au-Cl complex nanostructures in silica shells,* Adv. Funct. Mater., 16 (2006), pp. 1679-1684.

[6] Y. L. Shi and T. Asefa, *Tailored core-shell-shell nanostructures: Sandwiching gold nanoparticles between silica cores and tunable silica shells*, Langmuir, 23 (2007), pp. 9455-9462.

[7] J. Lee, J. C. Park and H. Song, *A nanoreactor framework of a Au@SiO_2 yolk/shell structure for catalytic reduction of p-nitrophenol*, Adv. Mater., 20 (2008), pp. 1523-1528.

[8] J. Y. Kim, S. B. Yoon and J. S. Yu, *Fabrication of nanocapsules with Au particles trapped inside carbon and silica nanoporous shells*, Chem. Commun. (2003), pp. 790-791.

[9] A. Kulak, S. A. Davis, E. Dujardin and S. Mann, *Controlled assembly of nanoparticle-containing gold and silica/gold nanocomposite spheroids with complex form,* Chem. Mater., 15 (2003), pp. 528-535.

[10] L. M. Liz-Marzan and P. Mulvaney, *The assembly of coated nanocrystal*, J. Phys. Chem. B, 107 (2003), pp. 7312-7326.

[11] H. P. Liang, L. J. Wan, C. L. Bai and L. Jiang, *Gold hollow nanospheres: Tunable surface plasmon resonance controlled by interior-cavity sizes*, J. Phys. Chem. B, 109 (2005), pp. 7795-7800.

[12] H. Hiramatsu and F. E. Osterloh, *pH-controlled assembly and disassembly of electrostatically linked CdSe-SiO_2 and Au-SiO_2 nanoparticle clusters*, Langmuir, 19 (2003), pp. 7003-7011.

[13] S. E. Park, M. Y. Park, P. K. Han and S. W. Lee, *The effect of pH-adjusted gold colloids on the formation of gold clusters over APTMS-coated silica cores*, Bull. Korean Chem. Soc., 27 (2006), pp. 1341-1345.

[14] L. Zhang, Y. G. Feng, L. Y. Wang, J. Y. Zhang, M. Chen and D. J. Qian, *Comparative studies between synthetic routes of SiO_2@Au composite nanoparticles,* Mater. Res. Bull., 42 (2007), pp. 1457-1467.

[15] F. Osterloh, H. Hiramatsu, R. Porter and T. Guo, *Alkanethiol-induced structural rearrangements in silica-gold core-shell-type nanoparticle clusters: An opportunity for chemical sensor engineering*, Langmuir, 20 (2004), pp. 5553-5558.

[16] B. Sadtler and A. Wei, *Spherical ensembles of gold nanoparticles on silica: electrostatic and size effects*, Chem. Commun. (2002), pp. 1604-1605.

[17] Y. Zhao, B. Sadtler, M. Lin, G. H. Hockerman and A. Wei, *Nanoprobe implantation into mammalian cells by cationic transfection*, Chem. Commun. (2004), pp. 784-785.

[18] S. L. Westcott, S. J. Oldenburg, T. R. Lee and N. J. Halas, *Formation and adsorbtion of clusters of gold nanoparticles onto functionalized silica nanoparticle surfaces*, Langmuir, 14 (1998), pp. 5396-5401.

[19] N. Phonthammachai and T. J. White, *One-step synthesis of highly dispersed gold nanocrystals on silica spheres*, Langmuir, 23 (2007), pp. 11421-11424.

[20] A. Ohnuma, R. Abe, T. Shibayama and B. Ohtani, *Heterodimeric particle assemblies: Preparation of anisotropically connected spherical silica particles via surface-bound gold nanoparticles*, Chem. Commun. (2007), pp. 3491-3493.

[21] C. G. Tian, B. D. Mao, E. B. Wang, Z. H. Kang, Y. L. Song, C. L. Wang and S. H. Li, *Simple strategy for preparation of core colloids modified with metal nanoparticles*, J. Phys. Chem. C, 111 (2007), pp. 3651-3657.

[22] S. J. Oldenberg, R. D. Averitt, S. L. Westcott and N. J. Halas, *Nanoengineering of optical resonances*, Chem. Phys. Lett., 288 (1998), pp. 243-247.

[23] M. S. Fleming and D. R. Walt, *Stability and exchange studies of alkanethiol monolayers on gold-nanoparticle-coated silica microspheres*, Langmuir, 17 (2001), pp. 4836-4843.

[24] J. C. Y. Kah, N. Phonthammachai, R. C. Y. Wan, J. Song, T. White, S. Mhaisalkar, I. Ahmad, C. Sheppard and M. Olivo, *Synthesis of gold nanoshells based on the deposition-precipitation process*, Gold Bull., 41 (2008), pp. 23-36.

[25] H. Wang, D. W. Brandl, P. Nordlander and N. J. Halas, *Plasmonic nanostructures: Artificial molecules*, Acc. Chem. Res., 40 (2007), pp. 53-62.

[26] X. H. Xia, Y. Liu, V. Backman and G. A. Ameer, *Engineering sub-100 nm multi-layer nanoshells*, Nanotechnology, 17 (2006), pp. 5435-5440.

[27] E. Prodan, C. Radloff, N. J. Halas and P. Nordlander, *A hybridization model for the plasmon response of complex nanostructures*, Science, 302 (2003), pp. 419-422.

[28] N. Harris, M. J. Ford, P. Mulvaney and M. B. Cortie, *Tunable infrared absorption by metal nanoparticles: The case for gold rods and shells*, Gold Bull., 41 (2008), pp. 5-14.

[29] S. Kalele, S. W. Gosavi, J. Urban and S. K. Kulkarni, *Nanoshell particles: synthesis, properties and applications*, Curr. Sci., 91 (2006), pp. 1038-1052.

[30] J. Kim, J. E. Lee, J. Lee, Y. Jang, S. W. Kim, K. An, H. H. Yu and T. Hyeon, *Generalized fabrication of multifunctional nanoparticle assemblies on silica spheres*, Angew. Chem. Int. Ed., 45 (2006), pp. 4789-4793.

[31] J. Kim, S. Park, J. E. Lee, S. M. Jin, J. H. Lee, I. S. Lee, I. Yang, J. S. Kim, S. K. Kim, M. H. Cho and T. Hyeon, *Designed fabrication of multifunctional magnetic gold nanoshells and their application to magnetic resonance imaging and photothermal therapy*, Angew. Chem. Int. Ed., 45 (2006), pp. 7754-7758.

[32] A. H. Lu, E. L. Salabas and F. Schuth, *Magnetic nanoparticles: Synthesis, protection, functionalization, and application*, Angew. Chem. Int. Ed., 46 (2007), pp. 1222-1244.

[33] M. Spasova, V. Salgueirino-Maceira, A. Schlachter, M. Hilgendorff, M. Giersig, L. M. Liz-Marzan and M. Farle, *Magnetic and optical tunable microspheres with a magnetite/gold nanoparticle shell*, J. Mater. Chem., 15 (2005), pp. 2095-2098.

[34] X. J. Ji, R. P. Shao, A. M. Elliott, R. J. Stafford, E. Esparza-Coss, J. A. Bankson, G. Liang, Z. P. Luo, K. Park, J. T. Markert and C. Li, *Bifunctional gold nanoshells with a superparamagnetic iron oxide-silica core suitable for both MR imaging and photothermal therapy*, J. Phys. Chem. C, 111 (2007), pp. 6245-6251.

[35] J. Lee, J. Yang, H. Ko, S. J. Oh, J. Kang, J. H. Son, K. Lee, S. W. Lee, H. G. Yoon, J. S. Suh, Y. M. Huh and S. Haam, *Multifunctional magnetic gold nanocomposites: Human epithelial cancer detection via magnetic resonance imaging and localized synchronous therapy*, Adv. Funct. Mater., 18 (2008), pp. 258-264.

[36] C. L. Fang, K. Qian, J. H. Zhu, S. B. Wang, X. X. Lv and S. H. Yu, *Monodisperse alpha-Fe_2O_3@SiO_2@Au core/shell nanocomposite spheres: synthesis, characterization and properties*, Nanotechnology, 19 (2008), pp. 1-7.

[37] W. S. Choi, H. Y. Koo and D. Y. Kim, *Scalable synthesis of chestnut-bur-like magnetic capsules loaded with size-controlled mono- or bimetallic cores*, Adv. Mater., 19 (2007), pp. 451-455.

[38] D. E. Lynch, Y. Nawaz and T. Bostrom, *Preparation of sub-micrometer silica shells using poly(1-methylpyrrol-2-ylsquaraine)*, Langmuir, 21 (2005), pp. 6572-6575.

[39] The λmax of the as prepared concentrated Au colloid was outside the range of the instrument.

[40] S. Begum, I. P. Jones, C. Jiao, D. E. Lynch and J. A. Preece, Unpublished work, pp.

[41] R. D. Badley, W. T. Ford, F. J. McEnroe and R. A. Assink, *Surface Modification Of Colloidal Silica*, Langmuir, 6 (1990), pp. 792-801.

[42] G. Frens, *Controlled Nucleation For Regulation Of Particle-Size In Monodisperse Gold Suspensions*, Nature-Physical Science, 241 (1973), pp. 20-22.

[43] The concentration of the Au colloid prepared using the original Frens procedure was too low for the purpose of this work. We found that APTMS treated hollow 'Si' spheres exposed to the Frens sol once were not densely covered with Au NPs. Therefore, using the Frens procedure we developed a procedure to prepare a more concentrated Au NP colloid.

[44] S. Kinge, M. Crego-Calama and D. N. Reinhoudt, *Self-assembling nanoparticles at surfaces and interfaces*, ChemPhysChem, 9 (2008), pp. 20-42.

[45] Through hypothesis tests we can show that the Au NPs prepared here (16.57 nm) have a similar average diameter as the Au NPs described by Frens (16 nm). We calculated a p-value of 0.0892 using the hypothesis test Ha ≠ Ho (where Ha= 16.57 nm, Ho= 16 nm) and the data in Figure 3b. The p-value 0.0892 does not fall into the rejection region ($p < 0.05$) of the standard normal distribution, so we can assume that Ha and Ho are similar.

[46] J. Turkevich, *Colloidal Gold. Part II: Colour, coagulation, adhesion, alloying and catalytic properties*, Gold Bull., 18 (1985), pp. 125-131.

[47] I. E. Sendroiu, S. F. L. Mertens and D. J. Schiffrin, *Plasmon interactions between gold nanoparticles in aqueous solution with controlled spatial separation*, PCCP, 8 (2006), pp. 1430-1436.

Table 1. Amounts of Au NPs reacted with APTMS-'Si' (0.5ml) to prepare Au-'Si'$_{A-D}$, and λ_{max} (of the Au NP surface plasmon band) from corresponding UV-vis spectra (Figure 7a)

Label	Au (ml)	λ_{max} (nm)
Au NP	-	522
Au-'Si'$_A$	0.66	524
Au-'Si'$_B$	4	541
Au-'Si'$_C$	8	553
Au-'Si'$_D$	16	570

Table 2. Amounts of Au NPs reacted with APTMS-'FeSi' (0.5ml) to prepare Au-'FeSi'$_{E-G}$, and λ_{max} (of the Au NP surface plasmon band) from corresponding UV-vis spectra (Figure 7b)

Label	Au (ml)	λ_{max} (nm)
Au NP	-	522
Au-'FeSi'$_E$	16	575
Au-'FeSi'$_F$	24	586
Au-'FeSi'$_G$	40	613

Scheme 1. Preparation of APTMS functionalised hollow spheres and Au NPs; and self-assembly of Au NPs onto APTMS coated hollow spheres at pH 4.5

Figure 1. JEOL 7000 FEG SEM secondary electron micrograph (acquired at 4 kV) of carbon coated (a) bare-'Si' (b) APTMS-'Si'

Figure 2. Histograms of zeta potential (mV) vs. pH for aqueous suspensions of (a) APTMS-'Si' and (b) APTMS-'FeSi'

Figure 3. (a) JEOL 1200 TEM bright field micrograph and (b) histogram of frequency vs. diameter (nm) of Au NPs

Figure 4. JEOL 1200 TEM bright field micrographs of ultra thin (80-100 nm) sections through Au-'Si' shells (Au-'Si'$_{A\text{-}D}$,

Table 1) embedded in Araldite resin

Figure 5. JEOL 1200 TEM bright field micrograph of ultra thin (80-100 nm) sections through Au-'Si' shells (Au-'Si'_D,

Table 1) embedded in Araldite resin showing a silica shell that has Au NPs adsorbed on the both sides of the shell wall

Figure 6. JEOL 1200 TEM bright field micrographs of ultra thin (80-100 nm) sections through Au-'FeSi' shells (a) and (b) Au-'FeSi'$_{E}$, (c) and (d) Au-'FeSi'$_{F}$, (e) and (f) Au-'FeSi'$_{G}$ (Table 2)

Figure 7. Normalised UV-vis spectra of (a) Au-'Si'$_{A-D}$ (

Table 1) and (b) Au-‘FeSi’$_{E\text{-}G}$ (Table 2)

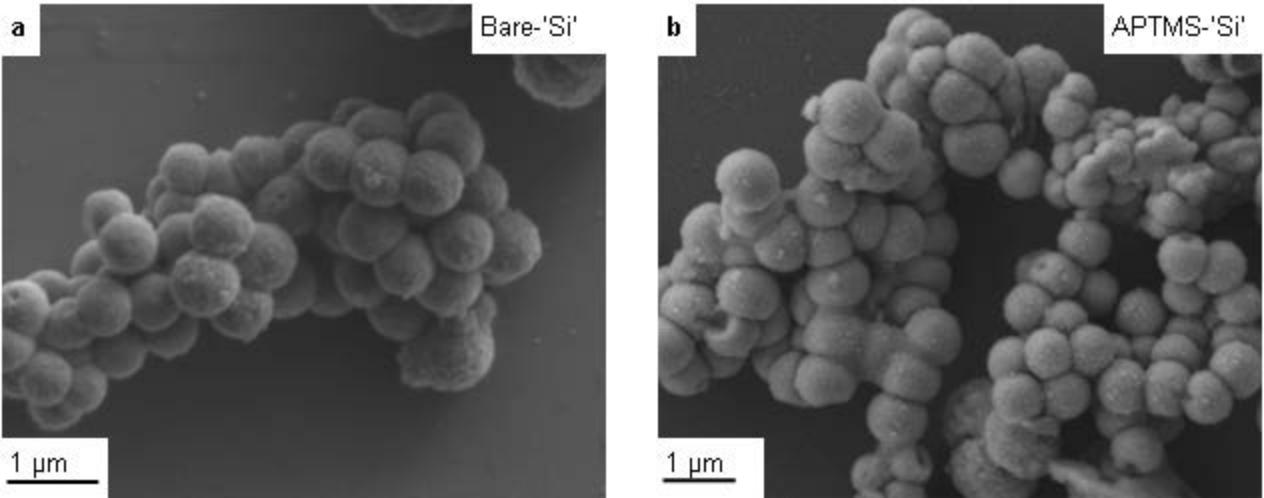
a
Bare-'Si'
1 µm
b
APTMS-'Si'
1 µm

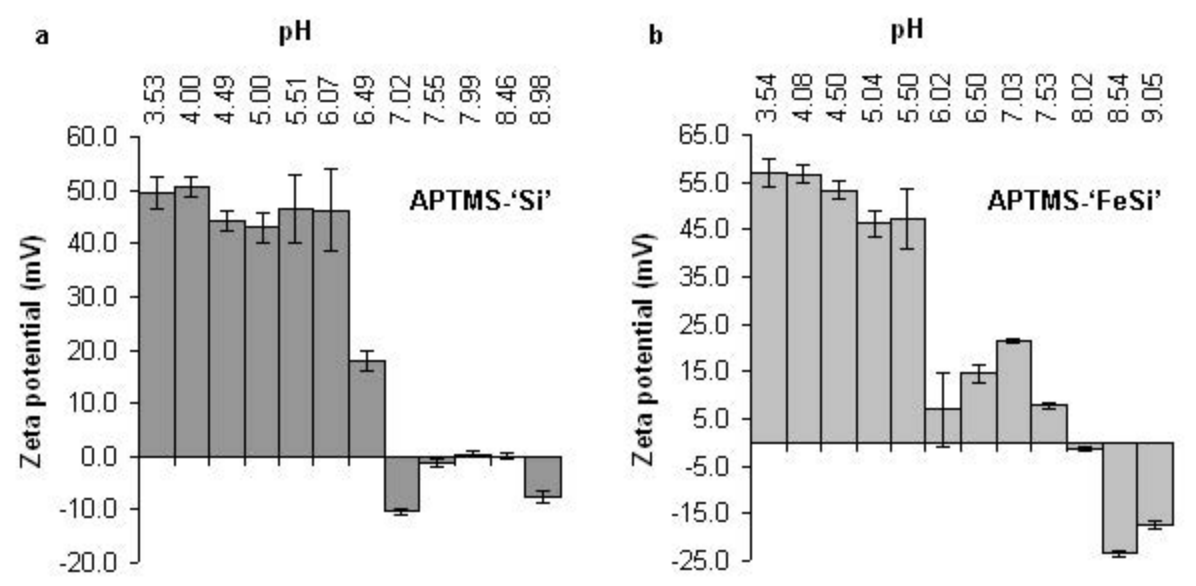
a
pH
3.53
4.00
4.49
5.00
5.51
6.07
6.49
7.02
7.55
7.99
8.46
8.98
60.0
50.0
40.0
30.0
20.0
10.0
0.0
-10.0
-20.0
Zeta potential (mV)
APTMS-'Si'
b
pH
3.54
4.08
4.50
5.04
5.50
6.02
6.50
7.03
7.53
8.02
8.54
9.05
65.0
55.0
45.0
35.0
25.0
15.0
5.0
-5.0
-15.0
-25.0
Zeta potential (mV)
APTMS-'FeSi'

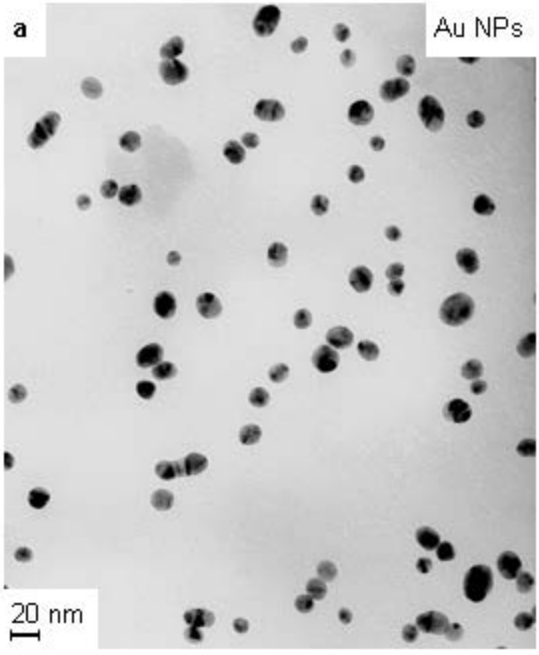
a
Au NPs
20 nm

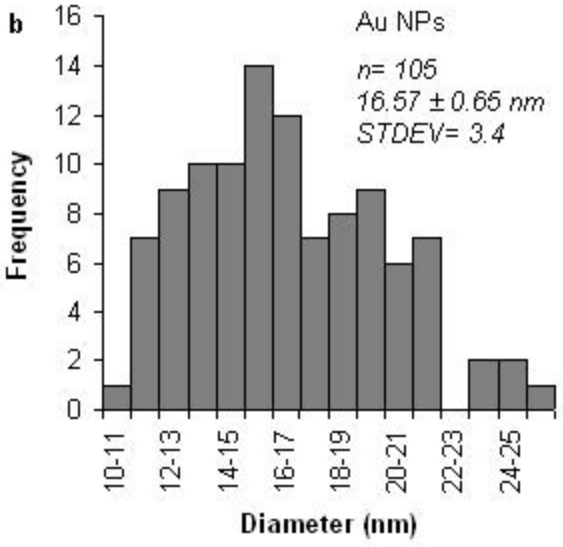
b
Au NPs
n= 105
16.57 ± 0.65 nm
STDEV= 3.4
Frequency
0
2
4
6
8
10
12
14
16
10-11
12-13
14-15
16-17
18-19
20-21
22-23
24-25
Diameter (nm)

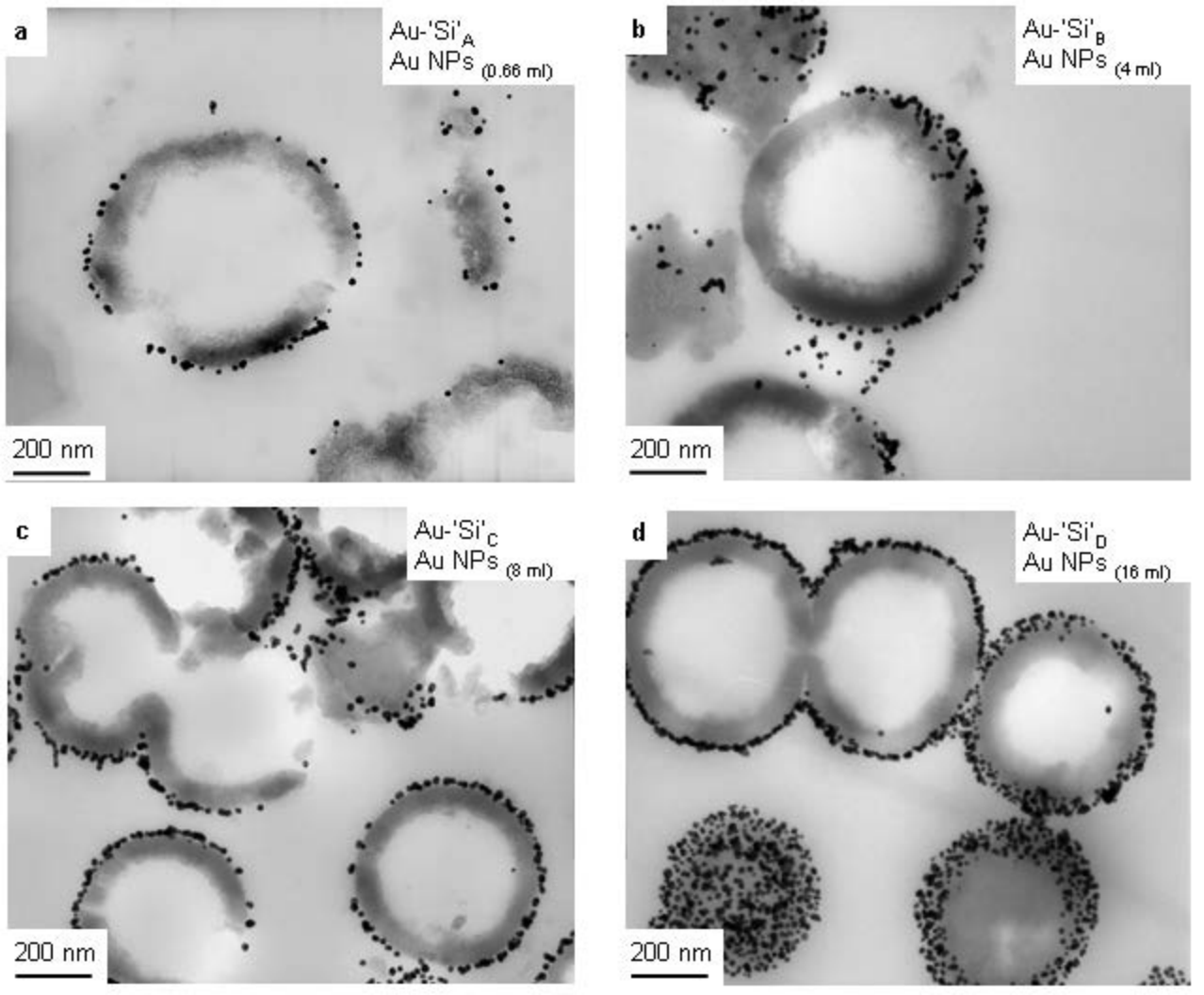
a
Au-'Si'A
Au NPs (0.66 ml)
200 nm
b
Au-'Si'B
Au NPs (4 ml)
200 nm
c
Au-'Si'C
Au NPs (8 ml)
200 nm
d
Au-'Si'D
Au NPs (16 ml)
200 nm

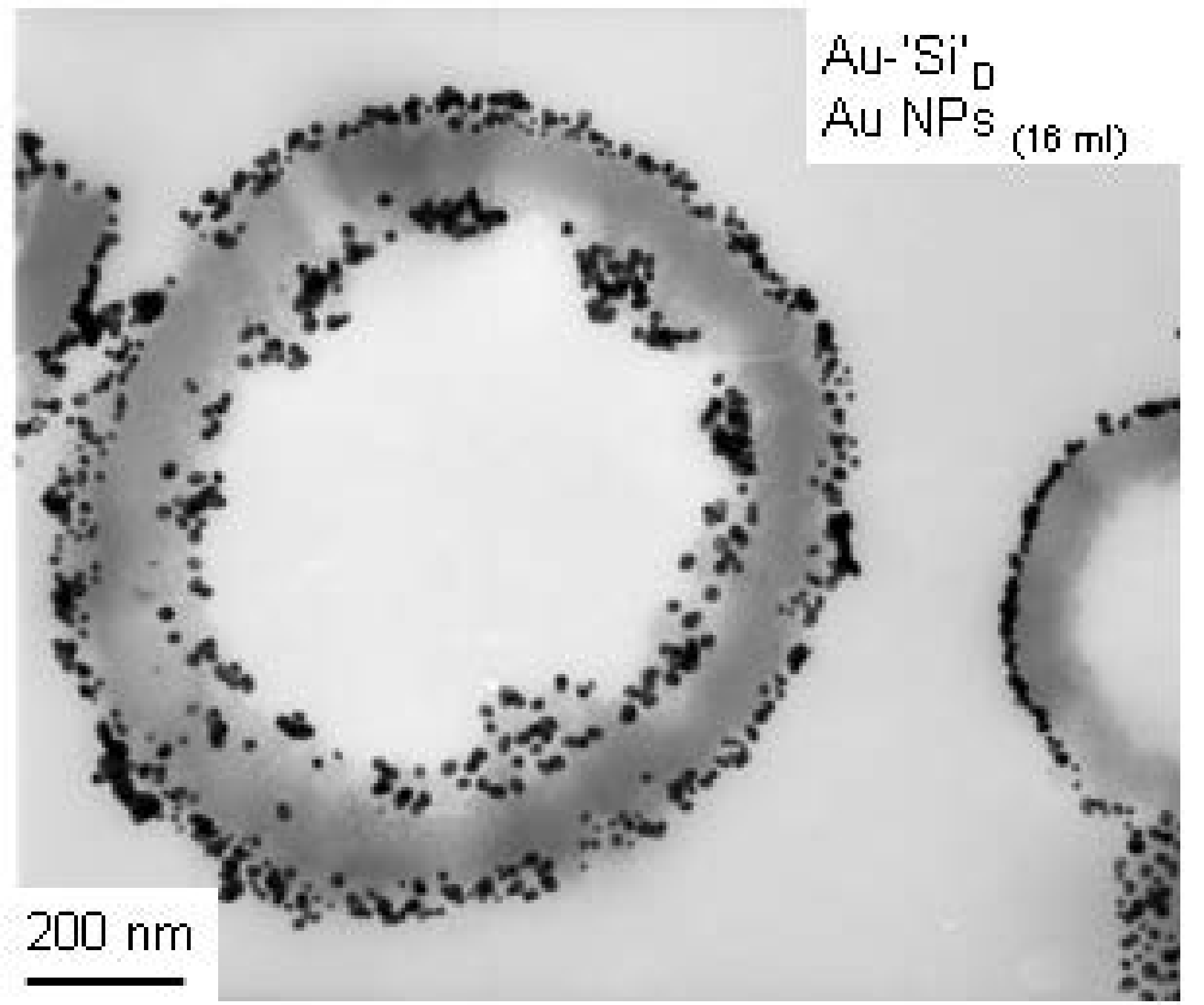
Au-'Si'D
Au NPs (16 ml)
200 nm

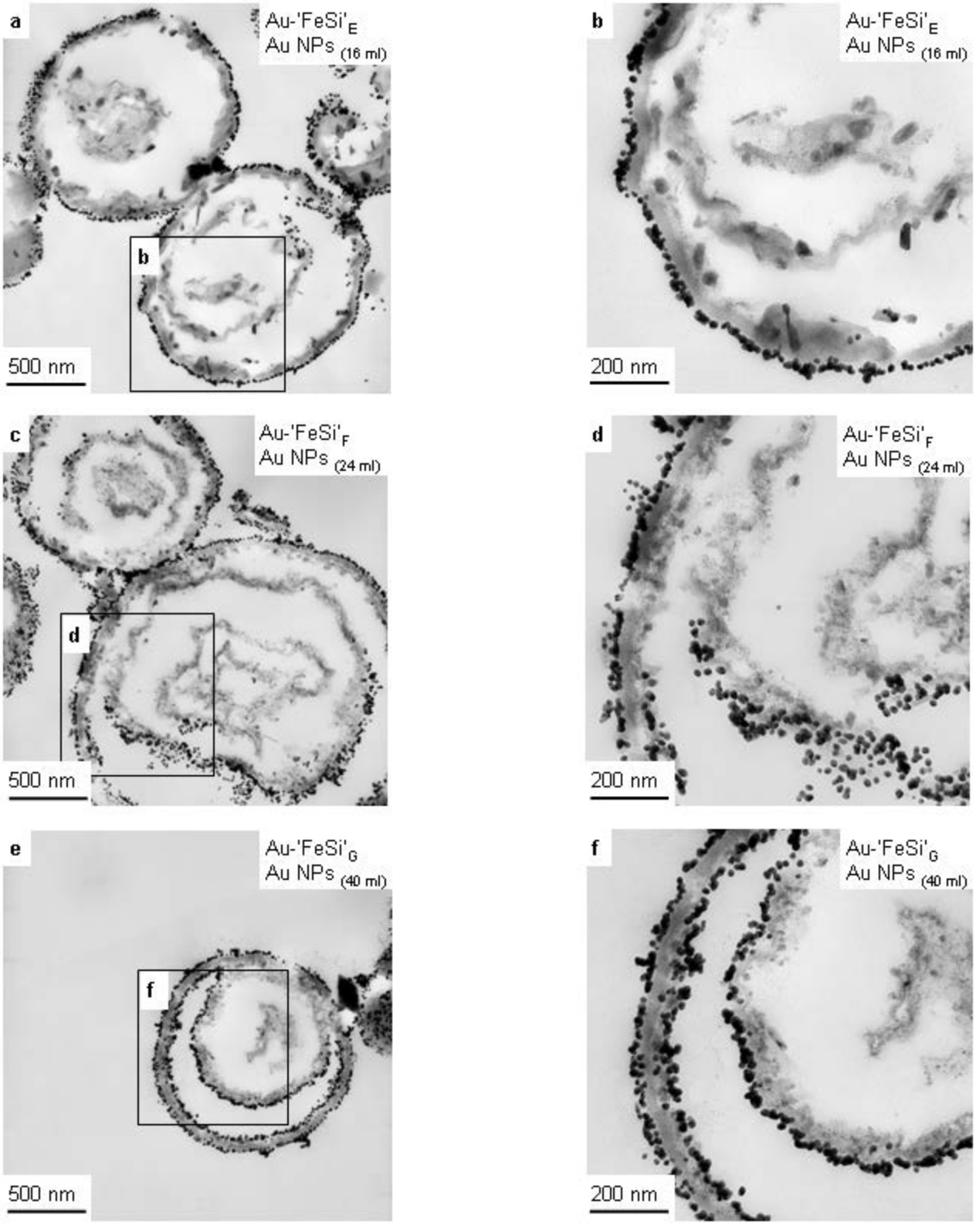
a
Au-'FeSi'E
Au NPs (16 ml)
b
500 nm
b
Au-'FeSi'E
Au NPs (16 ml)
200 nm
c
Au-'FeSi'F
Au NPs (24 ml)
d
500 nm
d
Au-'FeSi'F
Au NPs (24 ml)
200 nm
e
Au-'FeSi'G
Au NPs (40 ml)
f
500 nm
f
Au-'FeSi'G
Au NPs (40 ml)
200 nm

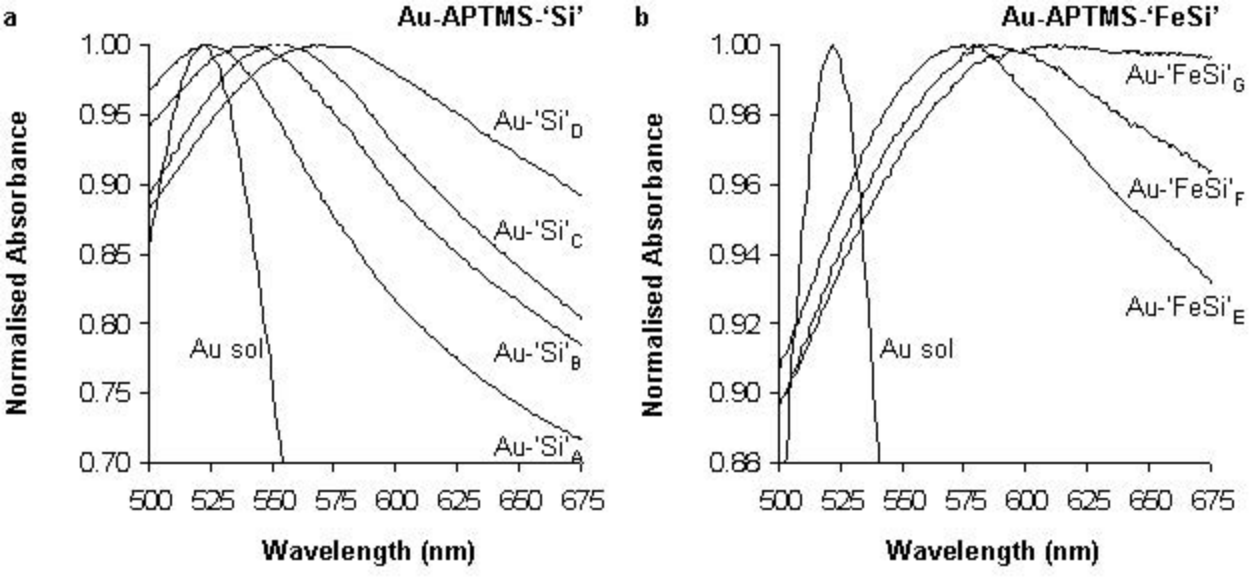
a
Au-APTMS-'Si'
Normalised Absorbance
1.00
0.95
0.90
0.85
0.80
0.75
0.70
Au-'Si'D
Au-'Si'C
Au-'Si'B
Au-'Si'A
Au sol
500 525 560 575 600 625 650 675
Wavelength (nm)
b
Au-APTMS-'FeSi'
Normalised Absorbance
1.00
0.98
0.96
0.94
0.92
0.90
0.88
Au-'FeSi'G
Au-'FeSi'F
Au-'FeSi'E
Au sol
500 525 560 575 600 625 650 675
Wavelength (nm)